Three irradiated and bloated hot Jupiters:

WASP-76b, WASP-82b & WASP-90b

R.G. West[1], J.-M. Almenara[2], D.R. Anderson[3], F. Bouchy[4], D. J. A. Brown[5], A. Collier Cameron[5], M. Deleuil[2], L. Delrez[6], A. P. Doyle[3], F. Faedi[1], A. Fumel[6], M. Gillon[6], G. Hébrard[4], C. Hellier[3], E. Jehin[6], M. Lendl[7], P.F.L. Maxted[3], F. Pepe[7], D. Pollacco[1], D. Queloz[7,8], D. Ségransan[7], B. Smalley[3], A.M.S. Smith[3,9], A.H.M.J. Triaud,[7,10]★, and S. Udry[7]

[1] Department of Physics, University of Warwick, Coventry CV4 7AL, UK
[2] Aix Marseille Université, CNRS, LAM (Laboratoire d'Astrophysique de Marseille) UMR 7326, 13388, Marseille, France
[3] Astrophysics Group, Keele University, Staffordshire, ST5 5BG, UK
[4] Institut d'Astrophysique de Paris, UMR 7095 CNRS, Université Pierre & Marie Curie, France; Observatoire de Haute-Provence, CNRS/OAMP, 04870, St Michel l'Observatoire, France
[5] SUPA, School of Physics and Astronomy, University of St. Andrews, North Haugh, Fife, KY16 9SS, UK
[6] Institut d'Astrophysique et de Géophysique, Université de Liège, Allée du 6 Août, 17, Bat. B5C, Liège 1, Belgium
[7] Observatoire astronomique de l'Université de Genève 51 ch. des Maillettes, 1290 Sauverny, Switzerland
[8] Cavendish Laboratory, J J Thomson Avenue, Cambridge, CB3 0HE, UK
[9] N. Copernicus Astronomical Centre, Polish Academy of Sciences, Bartycka 18, 00-716 Warsaw, Poland
[10] Department of Physics and Kavli Institute for Astrophysics & Space Research, Massachusetts Institute of Technology, Cambridge, MA 02139, USA

ABSTRACT

We report three new transiting hot-Jupiter planets discovered from the WASP surveys combined with radial velocities from OHP/SOPHIE and Euler/CORALIE and photometry from Euler and TRAPPIST. All three planets are inflated, with radii 1.7–1.8 R_{Jup}. All orbit hot stars, F5–F7, and all three stars have evolved, post-MS radii (1.7–2.2 $R_\odot$). Thus the three planets, with orbits of 1.8–3.9 d, are among the most irradiated planets known. This reinforces the correlation between inflated planets and stellar irradiation.

Key words. stars: individual (WASP-76; BD+01 316) – stars: individual (WASP-82) – stars: individual (WASP-90) — planetary systems

1. Introduction

The naive expectation that a Jupiter-mass planet would have a one-Jupiter radius has been replaced by the realisation that many of the hot Jupiters found by transit surveys have inflated radii. Planets as large as ∼ 2 R_{Jup} have been found (e.g. WASP-17b, Anderson et al. 2010; HAT-P-32b, Hartman et al. 2011).

It is also apparent that inflated planets are found preferentially around hot stars. For example Hartman et al. 2012 reported three new HAT-discovered planets, with radii of 1.6–1.7 R_{Jup}, all transiting F stars. Here we continue this theme by announcing three new hot Jupiters, again all inflated and all orbiting F stars.

For a discussion of the radii of transiting exoplanets we refer the reader to the recent paper by Weiss et al. (2013). It seems clear that stellar irradiation plays a large role in inflating hot Jupiters, since no inflated planets are known that receive less than 2×10^8 erg s^{-1} cm^{-2} (Miller & Fortney 2011; Demory & Seager 2011). There is also an extensive literature discussing other mechanisms for inflating hot Jupiters, such as tidal dissipation (e.g. Leconte et al. 2010, and references therein) and Ohmic dissipation (e.g. Batygin & Stevenson 2010).

2. Observations

The three transiting-planet systems reported here are near the equator, and so have been observed by both the SuperWASP-North camera array on La Palma and by WASP-South at Sutherland in South Africa. Our methods all follow closely to those in previous WASP discovery papers. The WASP camera arrays are described in Pollacco et al. (2006) while our planet-hunting methods are described in Collier-Cameron et al. (2007a) and Pollacco et al. (2007).

Equatorial WASP candidates are followed up by obtaining radial velocities using the SOPHIE spectrograph on the 1.93-m telescope at OHP (as described in, e.g., Hébrard et al. 2013) and the CORALIE spectrograph on the 1.2-m Euler telescope at La Silla (e.g., Triaud et al. 2013). Higher-quality lightcurves of transits are obtained using EulerCAM on the 1.2-m telescope (e.g., Lendl et al. 2013) and the robotic TRAPPIST photometer at La Silla (e.g., Gillon et al. 2013). The observations for our three new planets are listed in Table 1.

3. The host stars

The stellar parameters for WASP-76, WASP-82 and WASP-90 were derived from the co-added RV spectra using the methods given in Doyle et al. (2013). The excitation balance of the Fe ɪ lines was used to determine the effective temperature (T_{eff}). The

---

★ Fellow of the Swiss National Science Foundation

Table 1. Observations

Facility	Date	
WASP-76:		
SuperWASP-North	2008 Sep–2010 Dec	12 800 points
WASP-South	2008 Jul–2009 Dec	7700 points
OHP/SOPHIE	2011 Sep–2011 Dec	9 RVs
Euler/CORALIE	2012 Feb–2012 Dec	8 RVs
TRAPPIST	2011 Nov 06	I filter
TRAPPIST	2012 Aug 25	I filter
EulerCAM	2012 Oct 13	Gunn r filter
TRAPPIST	2012 Oct 31	I filter
TRAPPIST	2012 Nov 20	I filter
WASP-82:		
SuperWASP-North	2008 Oct–2011 Feb	15 100 points
WASP-South	2008 Oct–2010 Jan	8600 points
OHP/SOPHIE	2011 Dec–2012 Feb	8 RVs
Euler/CORALIE	2012 Feb–2013 Mar	20 RVs
EulerCAM	2012 Nov 20	Gunn r filter
WASP-90:		
SuperWASP-North	2004 May–2010 Oct	40 800 points
WASP-South	2008 Jun–2009 Oct	12 200 points
Euler/CORALIE	2011 Oct–2012 Sep	15 RVs
TRAPPIST	2012 Jun 03	$I + z$ filter
EulerCAM	2012 Jul 28	Gunn r filter
TRAPPIST	2012 Sep 13	$I + z$ filter
EulerCAM	2013 Jun 10	Gunn r filter

surface gravity (log g) was determined from the ionisation balance of Fe I and Fe II. The Ca I line at 6439Å and the Na I D lines were also used as log g diagnostics. Values of microturbulence (ξ_t) were obtained by requiring a null-dependence on abundance with equivalent width. The elemental abundances were determined from equivalent width measurements of several unblended lines. The quoted error estimates include that given by the uncertainties in T_{eff} and log g, as well as the scatter due to measurement and atomic data uncertainties. The projected stellar rotation velocity ($v \sin I$) was determined by fitting the profiles of several unblended Fe I lines. Macroturbulence was obtained from the calibration by Bruntt et al. (2010).

For WASP-76, the rotation rate ($P = 17.6 \pm 4.0$ d) implied by the $v \sin I$ (assuming that the spin axis is perpendicular to us) gives a gyrochronological age of $5.3^{+6.1}_{-2.9}$ Gyr using the Barnes (2007) relation. The lithium age of several Gyr, estimated using results in Sestito & Randich (2005), is consistent. For WASP-90, the rotation rate ($P = 11.1 \pm 1.6$ d) implied by the $v \sin I$ gives a gyrochronological age of $4.4^{+8.4}_{-2.4}$ Gyr. The T_{eff} of this star is close to the lithium-gap (Böhm-Vitense, 2004), and thus the lack of any detectable lithium in this star does not provide a usable age constraint. WASP-82 is too hot for reliable gyrochronological or lithium ages.

We list in Tables 2–4 the proper motions of the three stars from the UCAC4 catalogue (Zacharias et al. 2013). These are compatible with the stars being from the local thin-disc population. We also searched the WASP photometry of each star for rotational modulations by using a sine-wave fitting algorithm as described by Maxted et al. (2011). For none of the three stars was a significant periodicity found (< 1 mmag at 95%-confidence).

4. System parameters

The radial-velocity and photometric data (Table 1) were combined in a simultaneous Markov-chain Monte-Carlo (MCMC) analysis to find the system parameters (see Collier Cameron et al.

2007b for an account of our methods). For limb-darkening we used the 4-parameter law from Claret (2000), and list the resulting parameters in Tables 2–4.

For WASP-76b and WASP-82b the radial-velocity data imply circular orbits with eccentricities less than 0.05 and 0.06 respectively. WASP-90 is a fainter star and WASP-90b is a lower-mass planet, so, while the data are again compatible with a circular orbit, the limit on the eccentricity is weaker at 0.5. For all three we enforced a circular orbit in the MCMC analysis (see Anderson et al. 2012 for the rationale for this). One of the WASP-82 RVs was taken during transit, and this point was given zero weight in the analysis. To translate transit and radial-velocity information (which give stellar density) into the star's mass and radius we need one additional mass–radius constraint. Here we use the calibration presented by Southworth (2011).

The fitted parameters were thus T_c, P, ΔF, T_{14}, b, K_1, where T_c is the epoch of mid-transit, P is the orbital period, ΔF is the fractional flux-deficit that would be observed during transit in the absence of limb-darkening, T_{14} is the total transit duration (from first to fourth contact), b is the impact parameter of the planet's path across the stellar disc, and K_1 is the stellar reflex velocity semi-amplitude. The resulting fits are reported in Tables 2 to 4.

5. Discussion

The three host stars, WASP-76, WASP-82 and WASP-90, are all F stars with temperatures of 6250–6500 K. Their metallicities ([Fe/H] = 0.1–0.2) and space velocities are compatible with the local thin-disk population. The stellar densities derived from the MCMC analysis, along with the temperatures from the spectral analysis, are shown on a modified H–R diagram in Fig. 4. All three stars have inflated radii ($R_* = 1.7$–2.2 R$_\odot$) and thus appear to have evolved significantly. The indicated ages of ∼ 2 Gyr are compatible with the estimates from gyrochronology (Section 2).

The three planets also all have inflated radii (1.7–1.8 R$_{Jup}$) and are thus bloated hot Jupiters. This is likely related to the high temperature and large radii of the host stars. Weiss et al. (2013) have shown that the radii of hot-Jupiter planets correlates well with their irradiation. Our three new planets fit their relationship, and are all at the extreme high-irradiation, high-radius end (their locations on Fig 14 of Weiss et al. being at fluxes 5.1, 5.2 and 2.9 ×10^9 erg cm^{-2}, s^{-1}, and radii 20.1, 18.4 and 19.6 R$_{Earth}$ for WASP-76b, WASP-82b and WASP-90b respectively). One caution, however, is that we have a bias against finding un-bloated hot Jupiter around evolved, high-radius stars, since the transit depths would be low.

Of particular note is that, at $V = 9.5$ and $R_P = 1.8$ R$_{Jup}$, WASP-76 is now the brightest known star transited by a planet larger than 1.5 R$_{Jup}$. WASP-82 is not far behind at $V = 10.1$ and $R_P = 1.7$ R$_{Jup}$, comparable to WASP-79 ($V = 10.1$, $R_P = 1.7$ R$_{Jup}$; Smalley et al. 2012, and KOI-13 ($V = 10.0$, $R_P = 1.8$ R$_{Jup}$; Santerne et al. 2012). Thus the new discoveries will be useful for studying bloated hot Jupiters. For example, Triaud (2011) suggests that the orbital inclinations of hot Jupiters are a function of system age. Given that radius changes of evolved systems give age constraints, WASP-76 and WASP-82 will be good systems for testing this idea. WASP-82 has a relatively small $v \sin I$ (Table 3) for its spectral type, which could indicate a mis-aligned orbit.
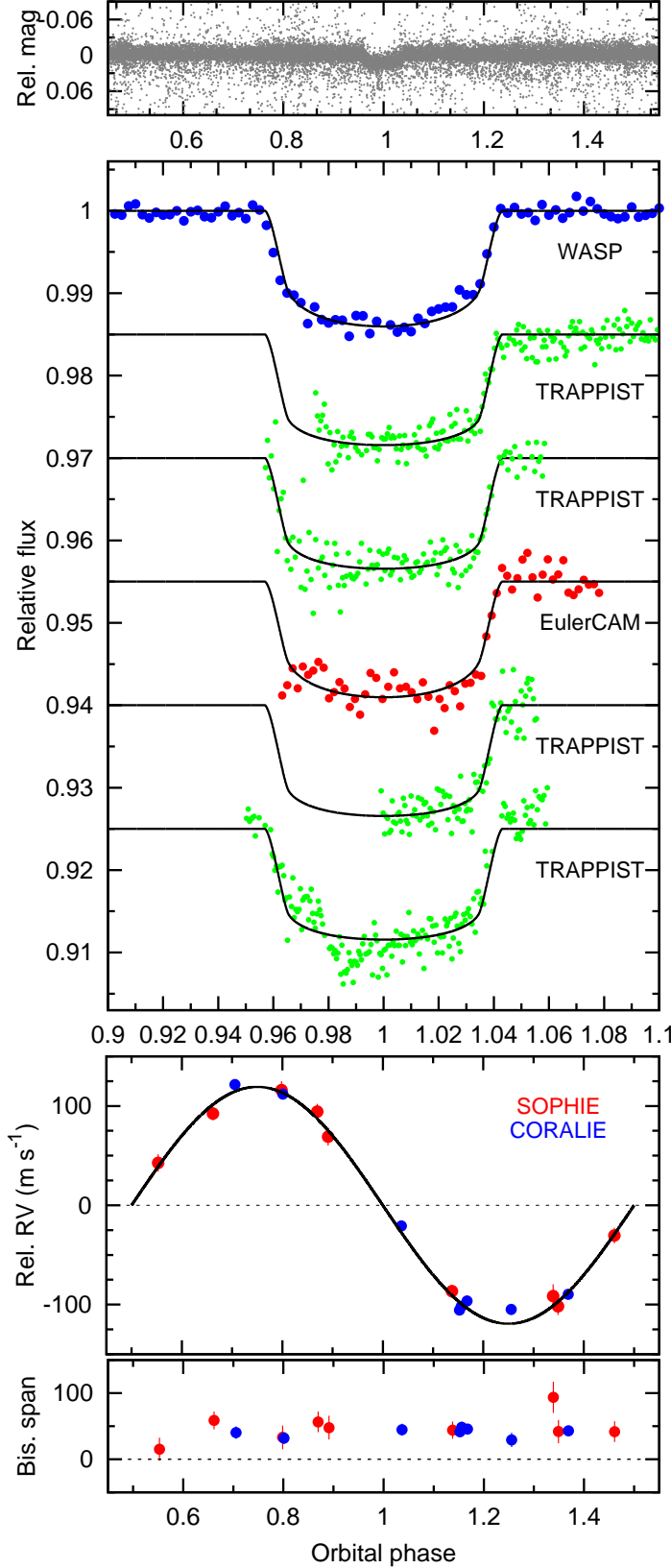
Table 2. System parameters for WASP-76.

BD+01 316
1SWASP J014631.86+024202.0
2MASS 01463185+0242019
RA = 01^{h}46^{m}31.86^s, Dec = +02°42′02.0″ (J2000)
V mag = 9.5
Rotational modulation   < 1 mmag (95%)
pm (RA) 46.6 ± 0.7 (Dec), −39.9 ± 0.6 mas/yr

Stellar parameters from spectroscopic analysis.	
Spectral type	F7
$T_{\rm eff}$ (K)	6250 ± 100
$\log g$	4.4 ± 0.1
$\xi_{\rm t}$ (km s^{-1})	1.4 ± 0.1
$v_{\rm mac}$ (km s^{-1})	4.0 ± 0.3
$v \sin I$ (km s^{-1})	3.3 ± 0.6
[Fe/H]	+0.23 ± 0.10
$\log A$(Li)	2.28 ± 0.10
Distance	120 ± 20 pc

Parameters from MCMC analysis.	
P (d)	1.809886 ± 0.000001
$T_{\rm c}$ (HJD) (UTC)	245 6107.85507 ± 0.00034
T_{14} (d)	0.1539 ± 0.0008
$T_{12} = T_{34}$ (d)	$0.0154^{+0.0008}_{-0.0003}$
$\Delta F = R_{\rm P}^2/R_*^2$	0.01189 ± 0.00016
b	$0.14^{+0.11}_{-0.09}$
i (°)	$88.0^{+1.3}_{-1.6}$
K_1 (km s^{-1})	0.1193 ± 0.0018
γ (km s^{-1})	−1.0733 ± 0.0002
e	0 (adopted) (<0.05 at 3σ)
M_* (M$_\odot$)	1.46 ± 0.07
R_* (R$_\odot$)	1.73 ± 0.04
$\log g_*$ (cgs)	4.128 ± 0.015
ρ_* ($\rho_\odot$)	$0.286^{+0.008}_{-0.018}$
$T_{\rm eff}$ (K)	6250 ± 100
$M_{\rm P}$ (M$_{\rm Jup}$)	0.92 ± 0.03
$R_{\rm P}$ (R$_{\rm Jup}$)	$1.83^{+0.06}_{-0.04}$
$\log g_{\rm P}$ (cgs)	2.80 ± 0.02
$\rho_{\rm P}$ ($\rho_{\rm J}$)	0.151 ± 0.010
a (AU)	0.0330 ± 0.0005
$T_{\rm P,A=0}$ (K)	2160 ± 40

Errors are 1σ; Limb-darkening coefficients were:
TRAPPIST z:
a1 = 0.683, a2 = −0.349, a3 = 0.565, a4 = −0.286
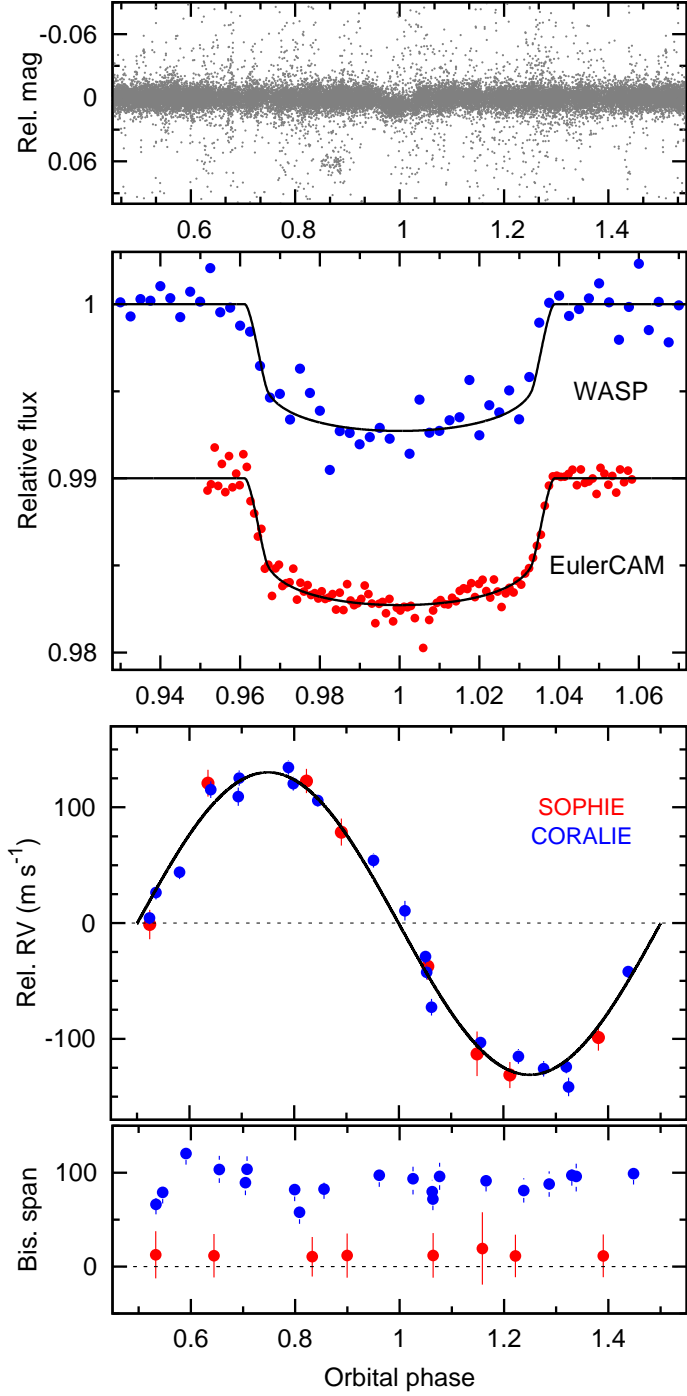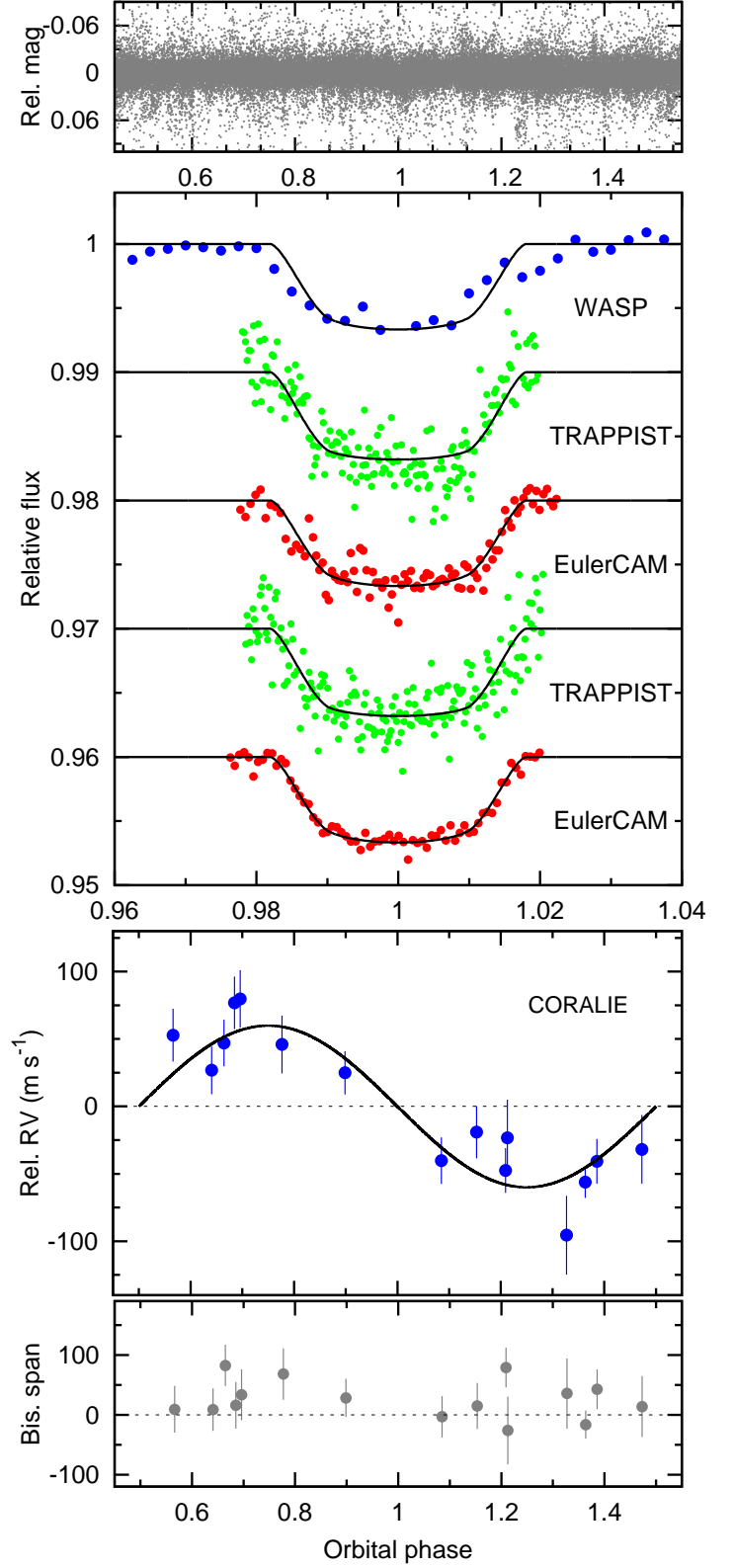EulerCAM r_G:
a1 = 0.593, a2 = 0.021, a3 = 0.327, a4 = −0.215

Fig. 1. WASP-76b discovery data: (Top) The WASP data folded on the transit period. (Second panel) The binned WASP data with (offset) the follow-up transit lightcurves (ordered from the top as in Table 1) together with the fitted MCMC model. (Third) The SOPHIE and CORALIE radial velocities with the fitted model. (Lowest) The bisector spans; the absence of any correlation with radial velocity is a check against transit mimics.

Fig. 2. WASP-82b discovery data (as for Fig. 1)

Table 3. System parameters for WASP-82.

1SWASP J045038.56+015338.1
2MASS 04503856+0153381
RA = $04^h50^m38.56^s$, Dec = $+01°53'38.1''$ (J2000)
V mag = 10.1
Rotational modulation   < 0.6 mmag (95%)
pm (RA) -17.5 ± 0.9 (Dec), -17.7 ± 0.7 mas/yr

Stellar parameters from spectroscopic analysis.	
Spectral type	F5
T_{eff} (K)	6500 ± 80
$\log g$	4.18 ± 0.09
ξ_t (km s^{-1})	1.5 ± 0.1
v_{mac} (km s^{-1})	5.0 ± 0.3
$v \sin I$ (km s^{-1})	2.6 ± 0.9
[Fe/H]	$+0.12 \pm 0.11$
$\log A(\mathrm{Li})$	3.11 ± 0.08
Distance	200 ± 30 pc

Parameters from MCMC analysis.	
P (d)	2.705782 ± 0.000003
T_c (HJD) (UTC)	$245\ 6157.9898 \pm 0.0005$
T_{14} (d)	0.2077 ± 0.0012
$T_{12} = T_{34}$ (d)	$0.0156^{+0.0012}_{-0.0004}$
$\Delta F = R_P^2/R_*^2$	0.00624 ± 0.00012
b	$0.16^{+0.14}_{-0.11}$
i (°)	$87.9^{+1.4}_{-1.9}$
K_1 (km s^{-1})	0.1307 ± 0.0019
γ (km s^{-1})	-23.62827 ± 0.00007
e	0 (adopted) (<0.06 at 3σ)
M_* (M$_\odot$)	1.63 ± 0.08
R_* (R$_\odot$)	$2.18^{+0.08}_{-0.05}$
$\log g_*$ (cgs)	$3.973^{+0.013}_{-0.02}$
ρ_* ($\rho_\odot$)	$0.158^{+0.006}_{-0.014}$
T_{eff} (K)	6490 ± 100
M_P (M$_{Jup}$)	1.24 ± 0.04
R_P (R$_{Jup}$)	$1.67^{+0.07}_{-0.05}$
$\log g_P$ (cgs)	$3.007^{+0.017}_{-0.032}$
ρ_P (ρ_J)	$0.266^{+0.017}_{-0.029}$
a (AU)	0.0447 ± 0.0007
$T_{P,A=0}$ (K)	2190 ± 40

Errors are 1σ; Limb-darkening coefficients were:
EulerCAM r_G:
a1 = 0.494, a2 = 0.424, a3 = −0.266, a4 = 0.0436

Table 4. System parameters for WASP-90.

1SWASP J210207.70+070323.7	
2MASS 01463185+0242019	
RA = 21^{h}02^{m}07.70^s, Dec = +07°03′23.7″ (J2000)	
V mag = 11.7	
Rotational modulation < 1 mmag (95%)	
pm (RA) −10.2 ± 1.4 (Dec), 8.1 ± 4.3 mas/yr	
Stellar parameters from spectroscopic analysis.	
Spectral type	F6
T_{eff} (K)	6440 ± 130
log g	4.32 ± 0.09
ξ_t (km s^{-1})	1.3 ± 0.2
v_{mac} (km s^{-1})	4.7±0.3
$v \sin I$ (km s^{-1})	6.0 ± 0.5
[Fe/H]	+0.11 ± 0.14
log A(Li)	<1.7
Distance	340 ± 60 pc
Parameters from MCMC analysis.	
P (d)	3.916243 ± 0.000003
T_c (HJD) (UTC)	245 6235.5639 ± 0.0005
T_{14} (d)	0.1398 ± 0.0022
$T_{12} = T_{34}$ (d)	0.033 ± 0.003
$\Delta F = R_P^2/R_*^2$	0.0071 ± 0.0002
b	0.841 ± 0.013
i (°)	82.1 ± 0.4
K_1 (km s^{-1})	0.060 ± 0.006
γ (km s^{-1})	4.361 ± 0.0003
e	0 (adopted) (<0.5 at 3σ)
M_* (M$_\odot$)	1.55 ± 0.10
R_* (R$_\odot$)	1.98 ± 0.09
log g_* (cgs)	4.033 ± 0.029
ρ_* ($\rho_\odot$)	0.20 ± 0.02
T_{eff} (K)	6430 ± 130
M_P (M$_{Jup}$)	0.63 ± 0.07
R_P (R$_{Jup}$)	1.63 ± 0.09
log g_P (cgs)	2.73 ± 0.06
ρ_P (ρ_J)	0.145 ± 0.027
a (AU)	0.0562 ± 0.0012
$T_{P,A=0}$ (K)	1840 ± 50
Errors are 1σ; Limb-darkening coefficients were:	
TRAPPIST $I + z$:	
a1 = 0.554, a2 = 0.041, a3 = 0.070, a4 = −0.086	
EulerCAM r_G:	
a1 = 0.476, a2 = 0.422, a3 = −0.226, a4 = 0.020	

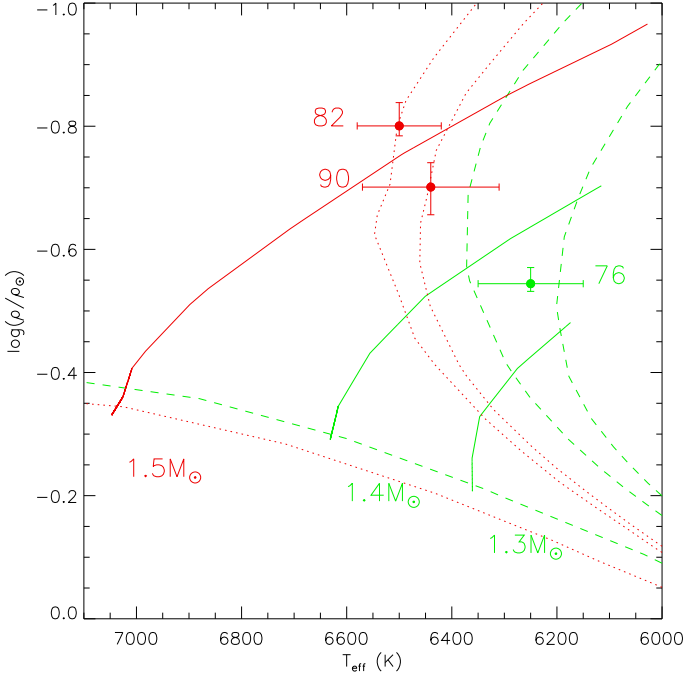**Fig. 3.** WASP-90b discovery data (as for Fig. 1)

Santerne, A.,Moutou, C., Barros, S. C. C. et al. 2012, A&A, 544, L12
Sestito P., Randich S., 2005, A&A, 442, 615
Smalley, B., Anderson, D. R., Collier-Cameron, A. et al, 2012, A&A, 547, A61
Smith A. M. S. et al. 2012, AJ, 143, 81
Southworth J., 2011, MNRAS, 417, 2166
Triaud, A. H. M. J., 2001, A&A, 534, L6
Triaud, A. H. M. J., Anderson, D. R., Collier Cameron, A. et al. 2013, A&A, 551, A80
Weiss, L. M., Marcy, G. W.,Rowe, J. F. et al. 2013, ApJ, 768, 14
Zacharias, N., Finch, C. T., Girard, T. M., Henden, A., Bartlett, J. L., Monet, D. G., Zacharias, M. I. 2013, AJ, 145, 44

Fig. 4. Evolutionary tracks on a modified H–R diagram (ρ versus T_{eff}). The green lines are for a metallicity of [Fe/H] = +0.19; the dashed lines are isochrones for 0.07, 2.0 and 2.5 Gyr; the solid lines are mass tracks for 1.3 $M_{\odot}$ and 1.4 $M_{\odot}$. The red lines are for a metallicity of [Fe/H] = +0.1, with the same isochrones, and the mass track for 1.5 $M_{\odot}$. The models are from Girardi et al. (2000).

References

Anderson, D. R., Collier Cameron, A., Gillon, M. et al. 2012, MNRAS, 422, 1988
Anderson, D. R., Hellier, C., Gillon, M. et al. 2010, ApJ, 709, 159
Asplund, M., Grevesse, N., Sauval, A.J., & Scott, P. 2009, ARA&A, 47, 481
Barnes, S.A. 2007, ApJ, 669, 1167
Batygin, K., Stevenson, D., J., 2010, ApJ, 714, L238
Böhm-Vitense, E. 2004, AJ, 128, 2435
Bruntt, H., Bedding, T.R., Quirion, P.-O., et al. 2010b, MNRAS, 405, 1907
Claret, A., 2000, A&A, 363, 1081
Collier Cameron, A., et al., 2007a , MNRAS, 375, 951
Collier Cameron, A., et al., 2007b, MNRAS, 380, 1230
Demory, B.-O., Seager, S., 2011, ApJS, 197, 12
Doyle, A.P., Smalley, B., Maxted, P.F.L., et al. 2013, MNRAS, 428, 3164
Gillon, M., Anderson, D. R., Collier-Cameron, A. et al. 2013, A&A, 552, A82
Girardi, L., Bressan, A., Bertelli, G., Chiosi, C. 2000, A&AS, 141, 371
Hartman, J. D., Bakos, G. Á., Béky, B. et al. 2012, AJ, 144, 139
Hartman, J. D., Bakos, G. Á., Torres, G. et al. 2011, ApJ, 742, 59
Hébrard, G., Collier Cameron, A., Brown, D. J. A. et al. 2013, A&A, 549, A134
Leconte, J., Chabrier, G., Baraffe, I., Levrard, B. 2010, A&A, 516, A64
Lendl, M., Anderson, D. R., Collier-Cameron, A. et al. 2012, A&A, 544, A72
Maxted, P.F.L. et al. 2011, PASP, 123, 547
Miller, N., Fortney, J. J. 2011, ApJ, 736, L29
Pollacco, D., et al., 2006, PASP, 118, 1407
Pollacco, D., et al., 2008, MNRAS, 385, 1576